N 62 10064

NASA TN D-1101

NASA TN D-1101

TECHNICAL NOTE

D-1101

INVESTIGATION OF TAPERED CIRCULAR REINFORCEMENTS AROUND CENTRAL HOLES IN FLAT SHEETS UNDER BIAXIAL LOADS IN THE ELASTIC RANGE

By Albert Kaufman, Peter T. Bizon,
and William C. Morgan

Lewis Research Center
Cleveland, Ohio

NATIONAL AERONAUTICS AND SPACE ADMINISTRATION

WASHINGTON February 1962

lG

NATIONAL AERONAUTICS AND SPACE ADMINISTRATION

TECHNICAL NOTE D-1101

E-1362

INVESTIGATION OF TAPERED CIRCULAR REINFORCEMENTS AROUND CENTRAL HOLES IN FLAT SHEETS UNDER BIAXIAL LOADS IN THE ELASTIC RANGE

By Albert Kaufman, Peter T. Bizon,
and William C. Morgan

SUMMARY

The effect of tapered ring reinforcements in reducing the stress concentrations around central holes in sheets under various biaxial stress fields in the elastic range was studied. The specimens were fabricated from plastic sheets as were the reinforcement rings. The rings were cemented symmetrically on each side of the sheet, and foil strain gages were mounted at various locations adjacent to the outer rim and at the inner rim of the reinforcements. Altogether, nine configurations were studied. These were tested in a biaxial testing machine, and the stress-concentration factors for 1:1, 1.5:1, 2:1, and 2.5:1 stress-field ratios were determined.

The best tapered reinforcements gave maximum stress-concentration factors of 1.00, 1.10, 1.17, and 1.20 for 1:1, 1.5:1, 2:1, and 2.5:1 stress-field ratios, respectively. These factors are slightly higher than those obtained with the best rectangular reinforcements of a previous investigation.

The initial effect of increasing the hub thickness or increasing the ring diameter is a sharp decrease in the stress-concentration factor at the inner rim; there is comparatively little effect on the stresses in the sheet. The results for the 1:1 stress field were compared with predictions from an analytical method of S. S. Manson, and good agreement was found for the tangential stresses at the inner rim and the effective stress-concentration factors in the sheet.

INTRODUCTION

The purpose of this investigation was to study the reinforcing effect of rings of triangular cross section (see fig. 1) around central

holes in biaxially loaded flat sheets. This is part of a more general experimental analysis of the problem of providing optimum reinforcements for openings in missile and space-vehicle tanks. The term "optimum reinforcement" implies one in which the maximum stress-concentration factor approaches unity as closely as possible. The best reinforcement of those tested will therefore be the one that most closely approximates an optimum reinforcement.

In a previous report (ref. 1) the stress concentrations around holes in flat sheets with reinforcements of rectangular cross section were investigated under various biaxial loading conditions. Generally the stress concentration at the inner rim of the hub could be reduced considerably below unity by increasing the hub size. However, the stress concentration in the sheet adjacent to the hub was not so easily reduced; in fact, the addition of material sometimes resulted in an increase in the stress-concentration factor. Therefore, an evaluation was made of the possibility that a better reinforcement could be obtained by using a triangular cross section, since the taper might result in a better utilization of the reinforcing material.

The investigation was carried out in a manner similar to that of reference 1. Each sheet of a methyl methacrylate plastic with a central hole was reinforced equally on each side with rings of triangular cross section. The specimens were tested under various combinations of biaxial loads, and the strains were measured with foil strain gages. The investigation reported herein was confined to the elastic range. Nine configurations were studied at stress-field ratios of 1:1, 1.5:1, 2:1, and 2.5:1, and the results were compared with those of reference 1 for rectangular reinforcements with the same volumes of reinforcing material. As in reference 1, only an 8:1 ratio of hole diameter to sheet thickness was considered because this is probably the smallest ratio that will be encountered in openings of missile tanks. Larger ratios would approximate more closely the plane-stress condition and would be expected to improve the reinforcement since bending stresses in the hub would be reduced. The experimental results for the 1:1 stress field were compared with results from a theoretical method (ref. 2).

SYMBOLS

C location at midpoint of hub inner rim on x-axis

H location in sheet adjacent to hub on x-axis

K effective stress-concentration factor

O location in sheet adjacent to hub at some angle from y-axis

H-1062

E-1362

V	location in sheet adjacent to hub on y-axis
X	ratio of outer to inner diameter of hub
Z	ratio of maximum hub thickness to sheet thickness
Θ	angle to location O as measured from y-axis
σ	normal stress, psi
τ	shear stress, psi

Subscripts:

C	location C
exp	experimental
H	location H
max	maximum
O	location O
r	radial direction
V	location V
x	direction of minimum nominal principal stress
y	direction of maximum nominal principal stress
z	direction normal to plane of sheet
θ	tangential direction
1	index for maximum nominal principal stress
2	index for minimum nominal principal stress
1r	first of duplicate back-to-back radial strain gages
2r	second of duplicate back-to-back radial strain gages
1θ	first of duplicate back-to-back tangential strain gages
2θ	second of duplicate back-to-back tangential strain gages

APPARATUS AND PROCEDURE

The testing of the specimens was carried out using the biaxial tensile machine described in reference 1 and shown in figure 2. Each of the specimens consisted of an 18- by 16-inch sheet of 1/8-inch methyl methacrylate plastic with a 1-inch-diameter central hole. Tapered rings of the same material were attached on each side of the plate around the hole with a cyanoacrylate cement. The rings had outer diameters of 1.4, 2.0, and 3.0 inches and maximum thicknesses of approximately one, two, and four times the plate thickness.

Strain gages were located back to back as shown in figure 1. The symbols in the figure are defined in the list of symbols. Perpendicularly oriented strain gages were located at V and H. Strains from corresponding gages at V_1 and V_2 and also at H_1 and H_2 were averaged. The equivalent of a 45° strain-gage rosette was located at O with the various gages of the rosette in different quadrants because of space limitations. Location O is meant to represent the location in the sheet where the stress-concentration factor is highest. This critical location will vary somewhat for each stress field and for each configuration. Nothing could be found in the literature that would afford a basis on which to predict the critical location in the sheet for tapered reinforcements. Therefore, for comparative purposes the angle Θ that was used was the same as in reference 1 for rectangular reinforcements of the same outer diameter. Thus, Θ was 45° for the 1.4-inch-diameter-ring configurations, 38° for the 2-inch-ring configurations, and 30° for the 3-inch-ring configurations. Circumferential and normal gages were located at C in the inner rim, which is the point of tangency with the direction of the maximum principal stress. Tangentially oriented gages (C_{θ}) were first mounted diametrically opposite at C; after the specimen had once been tested these were removed, a pair of normally oriented gages (C_z) was mounted in their place, and the test was repeated. The strain-gage output was recorded on an automatic multichannel recorder with an accuracy of ±1 percent.

The experimental procedure, which is described in more detail in reference 1, is summarized here. A calibration sheet with strain gages mounted on it but no reinforcement or central hole was initially tested in the machine. From this specimen the loadings required to give 1:1, 1.5:1, 2:1, and 2.5:1 stress-field ratios were determined.

The reinforced specimens were tested at four loadings, a zero reading being taken before and after each loading. The strain data were then processed by an electronic computer that corrected for zero drift, checked the linearity of the strains with load, and determined the stresses and stress-concentration factors at each point. The stress-concentration factors were computed using the effective stress based on

the von Mises energy theory. The equation for the effective stress-concentration factor at locations V, H, and O is

$$K = \sqrt{\frac{\sigma_\theta^2 + \sigma_r^2 - \sigma_r\sigma_\theta + 3\tau_{r\theta}^2}{\sigma_1^2 + \sigma_2^2 - \sigma_1\sigma_2}}$$

For location C, the stress normal to the plane of the sheet σ_z will be substituted for σ_r in the equation.

E-1362

RESULTS AND DISCUSSION

The experimental effective stress-concentration factors at locations C, V, H, and O are compiled in table I for each of the nine configurations that were studied at 1:1, 1.5:1, 2:1, and 2.5:1 stress-field ratios. For the 1:1 stress field, K_V, K_H, and K_O should be the same, and the differences among them are some indication of the experimental error for the particular configuration. The worst discrepancy occurred with the $X = 1.4$, $Z = 5.15$ reinforcement in the 1:1 stress field, in which the stress-concentration factor in the sheet varied from 0.98 to 1.06, a spread of about ±4 percent from the average value.

An explanation is required for the stress-concentration factors for location C for the $X = 1.4$, $Z = 3.01$ configuration. This specimen failed before the strains at C normal to the plane of the sheet could be obtained for any of the four stress-field ratios. These strains were obtained by interpolation from other data for $X = 1.4$ reinforcements and for an unreinforced specimen. The effect of including the interpolated bending stresses compared with ignoring them was an increase of approximately 5 percent in the effective stress-concentration factors for the various stress-field ratios.

Experimental Stress-Concentration Factors in Hub and Sheet

In figure 3 the effective stress-concentration factors at C are plotted against Z for each of the four stress-field ratios that were studied. In each part of the figure the curves for the $X = 1.4$, 2.0, and 3.0 reinforcements are extrapolated to the theoretical stress-concentration factor at $Z = 1$ corresponding to the unreinforced condition. Thus, all the curves for the 1:1 stress-field ratio (fig. 3(a)) converge to 2.000, for the 1.5:1 stress field (fig. 3(b)) to 2.646, for the 2:1 stress field (fig. 3(c)) to 2.886, and for the 2.5:1 stress field (fig. 3(d)) to 2.983.

The general trend of all the curves in figure 3 is for the stress-concentration factor at C to decrease considerably as the hub thickness initially increases and then to level out. In figure 3(a) the $X = 1.4$ curve seems to rise slightly as Z is increased from 5 to 9. However, the stress-concentration factors for $Z = 5$ and 9 are so close that the seeming rise in the curve may be nonexistent and may merely be the result of experimental error.

The effective stress-concentration factors in the sheet adjacent to the hub at locations V, O, and H are shown in figure 4. For the 1:1 stress-field ratio (fig. 4(a)) the experimental values of K_V, K_H, and K_O were averaged because the stress-concentration factor should be the same everywhere around the circumference. The maximum spread from the average (of the values) was about 5 percent. The curves of figure 4 were extrapolated to the theoretical stress-concentration factor for an unreinforced hole ($Z = 1$) for the particular location and stress-field ratio.

Locations of Maximum Stress-Concentration Factors

In figure 5 the maximum measured stress-concentration factors in the hub (location C) and in the sheet (location V, O, or H, whichever is greatest) are plotted against X. The results for the $Z = 3$, 5, and 9 configurations are shown in figures 5(a), (b), and (c), respectively. The data points in figure 5 were obtained by cross-plotting from figures 3 and 4 and do not necessarily represent the original data. The data points were used in figure 5 only to indicate the stress-field ratios and the locations of the maximum stresses in the specimens. Again all curves were extrapolated to the theoretical values at $X = 1$.

For a constant hub thickness and stress-field ratio, the maximum stress-concentration factor in the sheet decreases rapidly at first as X is increased, reaches a minimum between X values of 1.7 and 2.0, and then increases gradually. The change in the maximum stress-concentration factor in the sheet at values of X greater than 1.4 is small compared with the change in K_C, which shows a continuous decrease as X is increased. The point in figure 5 at which a dashed curve crosses a corresponding solid curve gives a configuration in which the maximum stress-concentration factors in the hub and in the sheet are equal. For configurations where X is larger, the maximum stress concentration was found in the sheet, and for lower values of X it was found in the hub.

E-1362

Selection of Reinforcement Geometry

Figures 3 to 5 were cross-plotted to give the three-dimensional graphs shown in figure 6. The dark shaded surfaces are configuration regions in which the highest stress concentration occurred in the sheet rather than the hub. These surfaces are essentially flat because of the relative insensitivity of the stress-concentration factor in the sheet to geometry changes. It is in these regions that the designer should choose a reinforcement configuration for the minimum stress concentration.

In figure 6(a) (for the 1:1 stress-field ratio) the dark region is approximately bounded by $X = 1.8$ and $Z = 4$, the maximum stress-concentration factor varying from 1.00 to 1.30. The best reinforcement is about $X = 2.0$ and $Z = 5$.

As the stress-field ratio increases, the range of suitable reinforcement geometries decreases, and the stress-concentration factors increase slightly. For the 1.5:1 stress-field ratio of figure 6(b), K_{max} for this range varies from 1.10 to 1.24 with the best reinforcement at $X = 2.0$, $Z = 9$.

The dark area in figure 6(c) (for the 2:1 stress-field ratio) has a K_{max} from 1.17 to 1.30. In figure 6(d) (for the 2.5:1 stress-field ratio) K_{max} varies from 1.20 to 1.30. Thus the 2:1 and the 2.5:1 stress-field ratios give approximately the same maximum stress-concentration factors. The best reinforcement geometry for both of these stress-field ratios is approximately $X = 3$, $Z = 5$.

Comparison of Experimental Results With Theoretical Analysis For 1:1 Stress Field

In figure 4(a) (for the 1:1 stress-field ratio) the experimental stress-concentration factors in the sheet are compared with theoretical curves obtained from the method of reference 2. The agreement for all three hub diameters is very good. The analysis of reference 2 is limited to a 1:1 stress field; therefore, comparisons could not be made for other stress-field ratios. The theoretical method assumes plane stress.

Theoretical and experimental stress-concentration factors based on the tangential stress at the hub inner rim are plotted in figure 7 and show good agreement. The comparison was not made with experimental effective stress-concentration factors because, for a hole-diameter to sheet-thickness ratio of 8:1, most of the tapered configurations that were investigated have high hub bending stresses normal to the plane of

the sheet; these stresses are not considered in reference 2. However, for larger ratios, where the bending stresses in the hub would be small, the method of reference 2 should predict the experimental effective stress-concentration factors adequately.

Comparison of Rectangular and Tapered Reinforcements

In figure 8 all the data from the tests of rectangular- and triangular-cross-section reinforcements are plotted on a volume basis. To make the abscissa nondimensional, the volume of the reinforcement rings is divided by the volume of material removed for the central hole in the flat sheet. The stress-concentration factor is the highest measured regardless of location.

Figure 8 indicates that the best rectangular reinforcements are somewhat better than the best triangular reinforcements because less reinforcing material is needed for the same stress-concentration factor and because lower stress-concentration factors can be attained. Based on the limited data for the tapered reinforcements, the superiority of the rectangular reinforcements is most obvious for the 2:1 (fig. 8(c)) and 2.5:1 (fig. 8(d)) stress-field ratios. For the 2:1 ratio the best rectangular reinforcement gave a maximum stress-concentration factor of 1.04 compared with about 1.17 for the tapered configurations. For the 2.5:1 stress-field ratio the best rectangular configuration gave a maximum stress-concentration factor of 1.08 compared with 1.20 for the best tapered configuration.

Size Effects and Other Considerations

In this paper only an 8:1 ratio of hole diameter to sheet thickness was studied. In most missile and space-vehicle tanks larger ratios will be involved. As the ratio becomes large, the reinforcement more nearly satisfies the plane-stress assumption because bending stresses in the hub are reduced for a given geometry. Since these bending stresses at location C are compressive, it can be expected that the stress concentration at C will also be reduced as the ratio of hole diameter to sheet thickness is increased. The three-dimensional effects in the hub do not affect the stress distribution in the sheet significantly.

The fact that the highest stress concentration for most of the tapered reinforcements occurs in the hub gives some importance to the size effect. It could mean that they would appear to better advantage relative to rectangular reinforcements at other ratios of hole diameter to sheet thickness. This is because the specimens with the best rectangular reinforcements generally were critical in the sheet and would not be materially affected by the size effect.

There is a possibility that higher stresses occurred at locations in the sheet other than where strain gages were located. The location angles θ were determined in reference 1 from a theoretical method that deals only with rectangular reinforcements. They were used in this investigation for purposes of comparison and because there were no better predictions available.

E-1362

CONCLUSIONS

The following conclusions can be drawn from the investigation of tapered circular reinforcements around central holes in flat sheets under various biaxial stress fields in the elastic range:

1. The best tapered configuration for the 1:1 stress-field ratio is $X = 2.0$, $Z = 5$ with $K_{max} = 1.00$ (where X is hub outer- to inner-diameter ratio, Z is maximum-hub-thickness to sheet-thickness ratio, and K_{max} is maximum stress-concentration factor). The best reinforcement for the 1.5:1 stress-field ratio is $X = 2.0$, $Z = 9$ with $K_{max} = 1.10$. For the 2:1 and 2.5:1 stress-field ratios the best reinforcement is about $X = 3.0$, $Z = 5$ with $K_{max} = 1.17$ and 1.20, respectively. These results were obtained for an 8:1 ratio of hole diameter to sheet thickness. Since the maximum stress-concentration factor occurred in the sheet in these particular configurations, there should be little size effect.

2. The best rectangular reinforcements were superior to the best triangular reinforcements because the maximum stress-concentration factors were slightly smaller and because less volume of material was needed for an equivalent reinforcement efficiency. The maximum stress-concentration factor that existed in the sheet when the reinforcement was of rectangular cross section was not reduced by tapering the hub.

3. A large reduction in the stress-concentration factor at the hub inner rim can be attained by increasing the hub thickness up to the point at which the maximum stress concentration occurs in the sheet. The effect of the hub thickness on the maximum stress-concentration factor in the sheet is relatively small for those configurations where the highest stress concentration is in the sheet.

4. A large reduction in the stress-concentration factor at the hub inner rim can be attained by increasing the hub outer diameter up to the point at which the stress-concentration factor reaches a minimum; it will increase gradually again as the diameter is increased further. The effect on the sheet is comparatively small for X values greater than 1.4.

5. Agreement between the experimental results and theoretical calculations from NACA Rep. 952 was good for the sheet and also for the tangential stress at the inner rim of the hub for the 1:1 stress field (the only stress field for which data from Rep. 952 are applicable).

Lewis Research Center
National Aeronautics and Space Administration
Cleveland, Ohio, December 12, 1961

E-1362

REFERENCES

1. Kaufman, Albert, Bizon, Peter T., and Morgan, William C.: Investigation of Circular Reinforcements of Rectangular Cross Section Around Central Holes in Flat Sheets Under Biaxial Loads in the Elastic Range. NASA TN D-1195, 1962.

2. Mason, S. S.: Direct Method of Design and Stress Analysis of Rotating Disks with Temperature Gradient. NACA Rep. 952, 1950. (Supersedes NACA TN 1957.)

E-1362

TABLE I. - EXPERIMENTAL DATA

Hub diameter ratio, X	Hub-sheet thickness ratio, Z	Stress-field ratio	Effective stress-concentration factor			
			K_C	K_V	K_H	K_O
1.4	3.01	1:1	[a]1.58	1.09	1.12	1.13
		1.5:1	[a]2.01	.89	1.23	1.16
		2:1	[a]2.15	.74	1.24	1.21
		2.5:1	[a]2.21	.64	1.22	1.25
	5.15	1:1	1.40	1.06	1.06	0.98
		1.5:1	1.81	.90	1.14	1.05
		2:1	1.95	.77	1.13	1.15
		2.5:1	2.01	.69	1.11	1.22
	8.84	1:1	1.43	1.04	1.02	1.03
		1.5:1	1.76	.88	1.06	1.11
		2:1	1.87	.76	1.04	1.21
		2.5:1	1.91	.69	1.01	1.29
2.0	2.86	1:1	1.18	0.96	0.98	1.00
		1.5:1	1.57	.90	.97	1.02
		2:1	1.72	.85	.94	1.06
		2.5:1	1.78	.81	.91	1.09
	4.71	1:1	0.99	1.01	1.01	0.96
		1.5:1	1.33	1.02	.94	.99
		2:1	1.45	1.00	.88	1.03
		2.5:1	1.51	.97	.83	1.06
	9.01	1:1	0.86	1.01	1.05	1.05
		1.5:1	1.09	1.06	.92	1.12
		2:1	1.18	1.06	.82	1.16
		2.5:1	1.22	1.04	.76	1.19
3.0	2.62	1:1	1.19	1.01	1.00	0.98
		1.5:1	1.56	1.04	.93	1.03
		2:1	1.70	1.04	.88	1.06
		2.5:1	1.76	1.03	.85	1.07
	4.92	1:1	0.82	1.06	1.07	1.06
		1.5:1	1.09	1.17	.92	1.14
		2:1	1.19	1.20	.82	1.18
		2.5:1	1.24	1.20	.77	1.19
	8.46	1:1	0.55	1.10	1.08	1.07
		1.5:1	.73	1.25	.87	1.15
		2:1	.80	1.29	.73	1.18
		2.5:1	.83	1.29	.66	1.19

[a]Value obtained by interpolation of normal (bending) strains from other data.

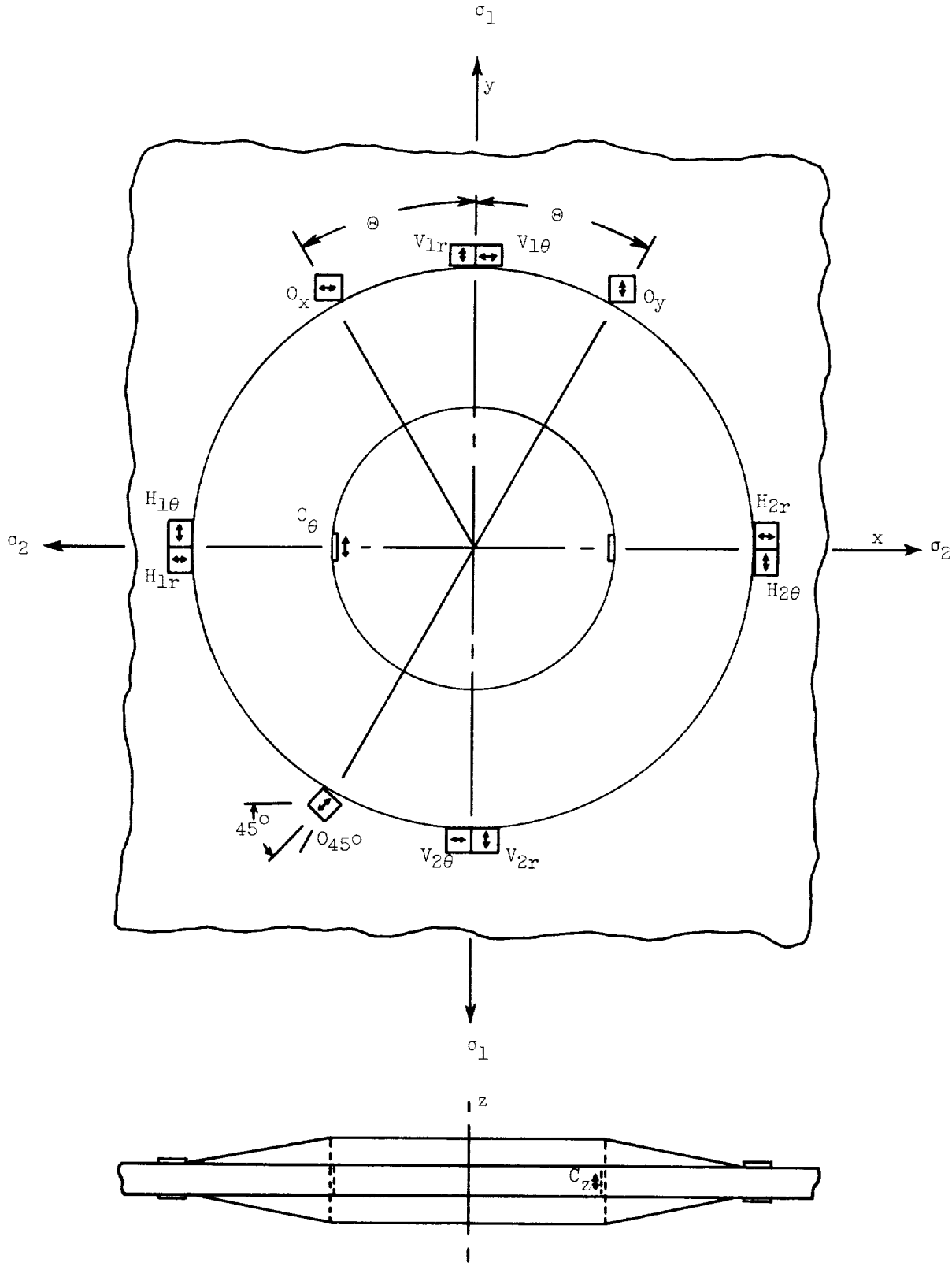

Figure 1. - Location and orientation of strain gages in reinforcement area of specimen.

E-1362

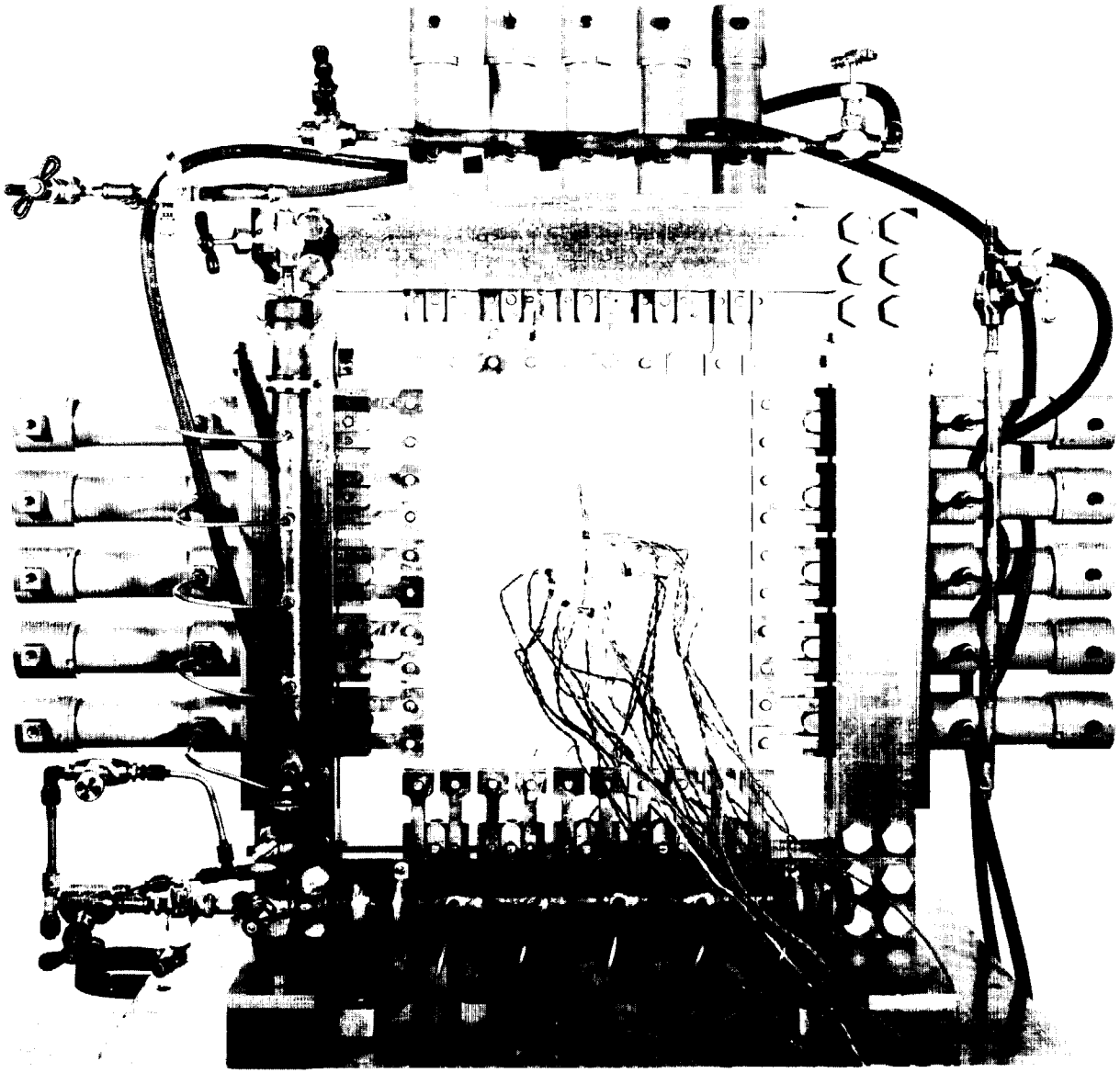

C-56820

Figure 2. - Biaxial tensile machine.

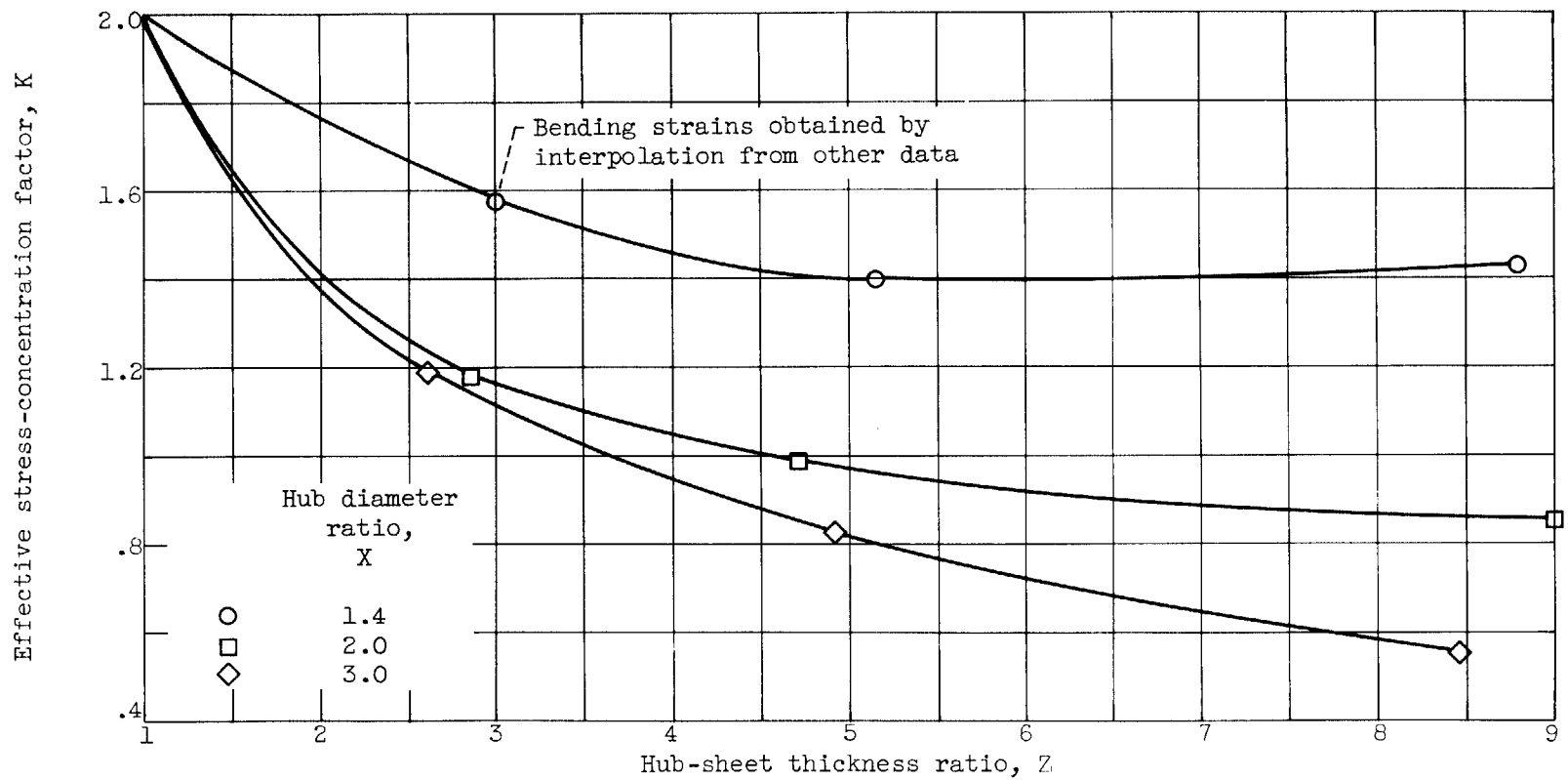

(a) Stress-field ratio, 1:1.

Figure 3. - Effective stress-concentration factors at location C.

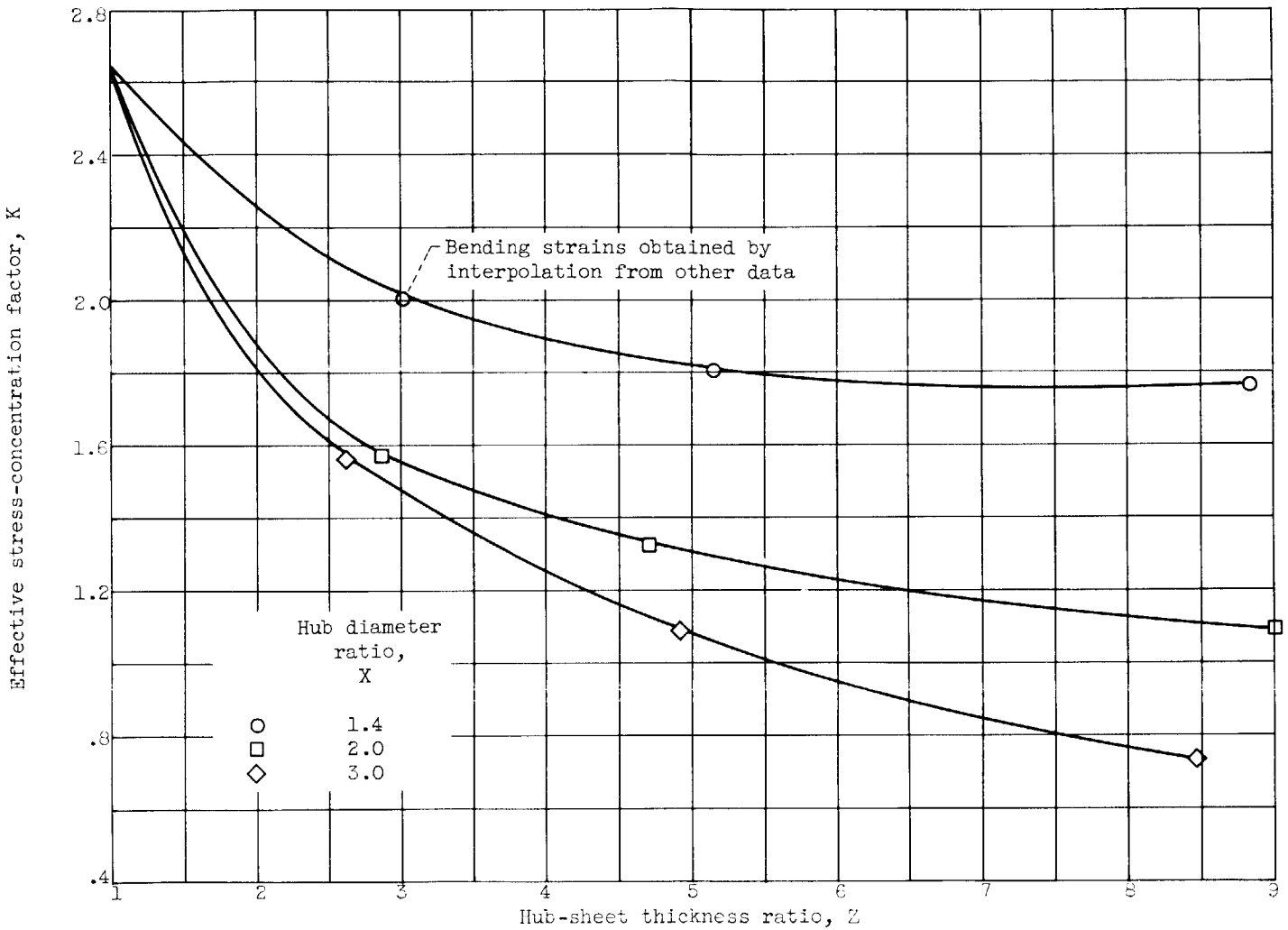

(b) Stress-field ratio, 1.5:1.

Figure 3. - Continued. Effective stress-concentration factors at location C.

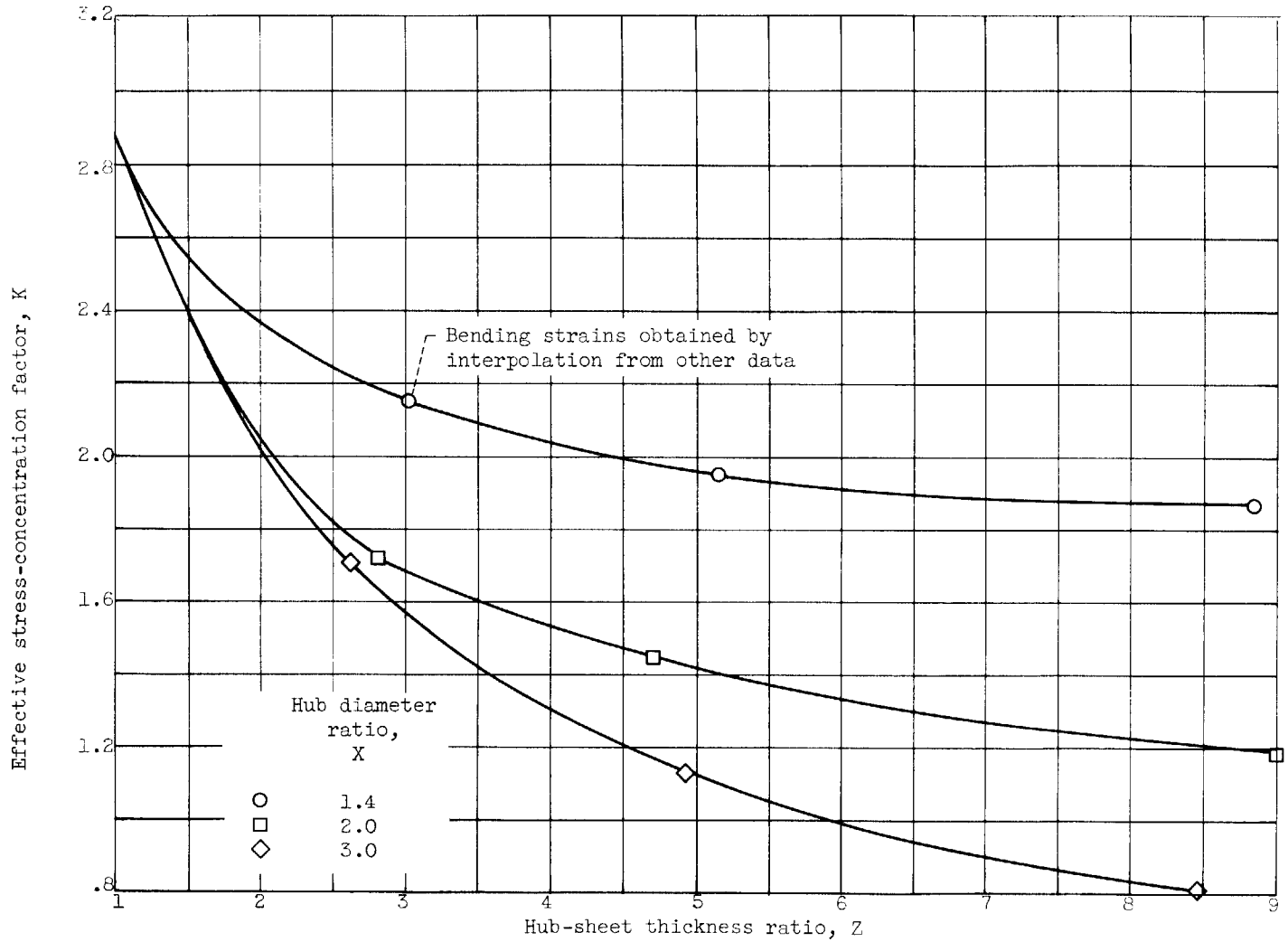

(c) Stress-field ratio, 2:1.

Figure 3. - Continued. Effective stress-concentration factors at location C.

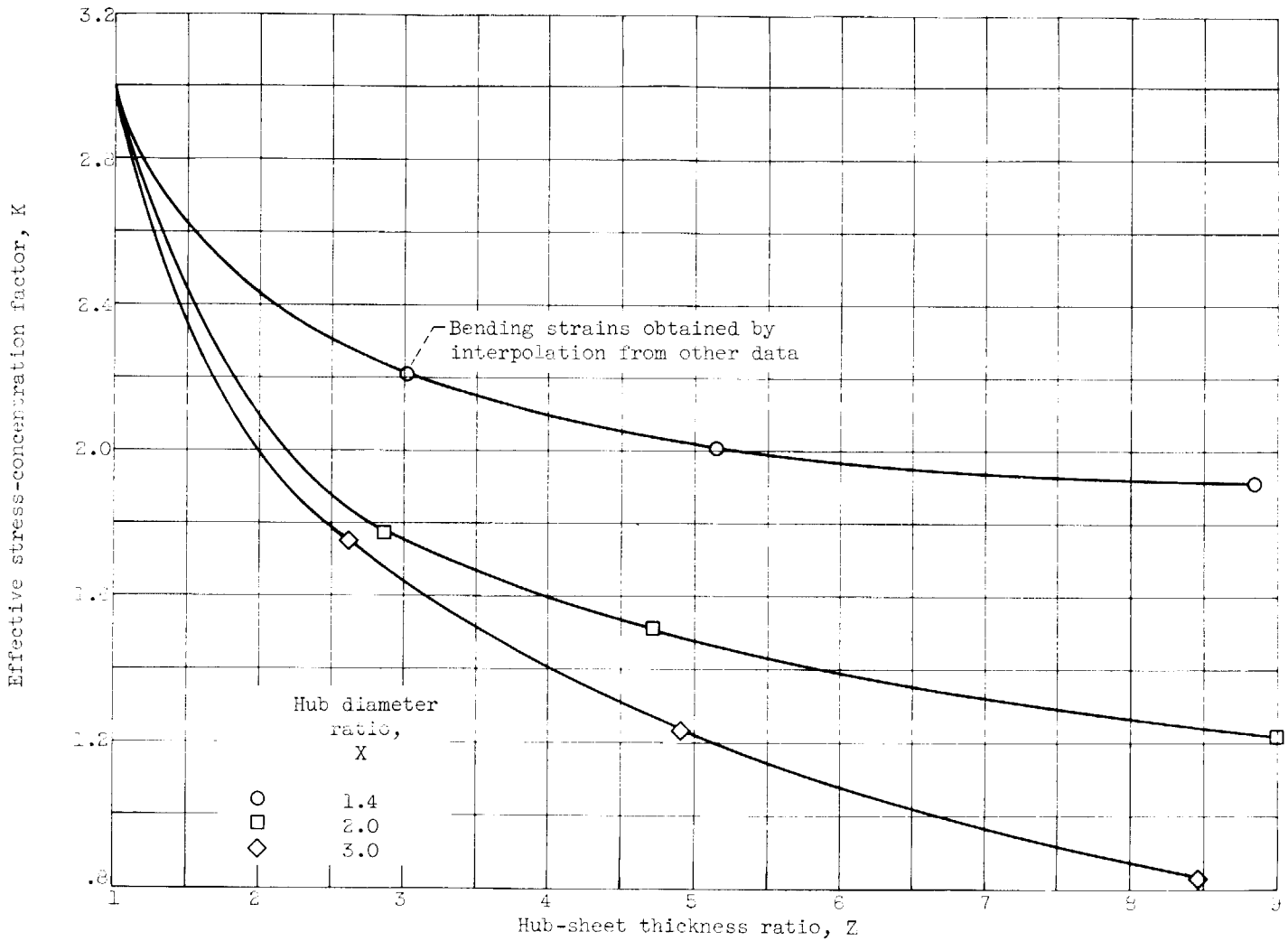

(d) Stress-field ratio, 2.5:1.

Figure 3. - Concluded. Effective stress-concentration factors at location C.

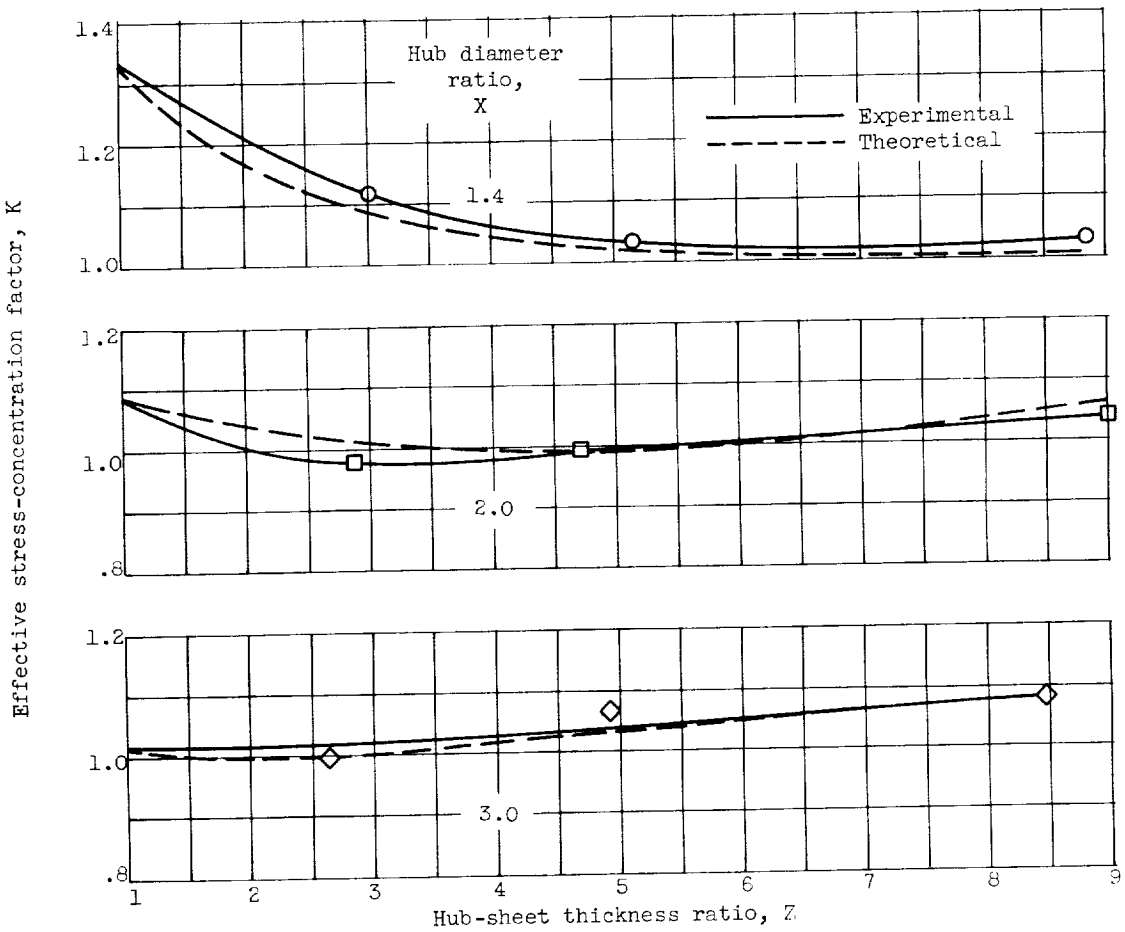

(a) Stress-field ratio, 1:1.

Figure 4. - Effective stress-concentration factors in sheet.

E-1362

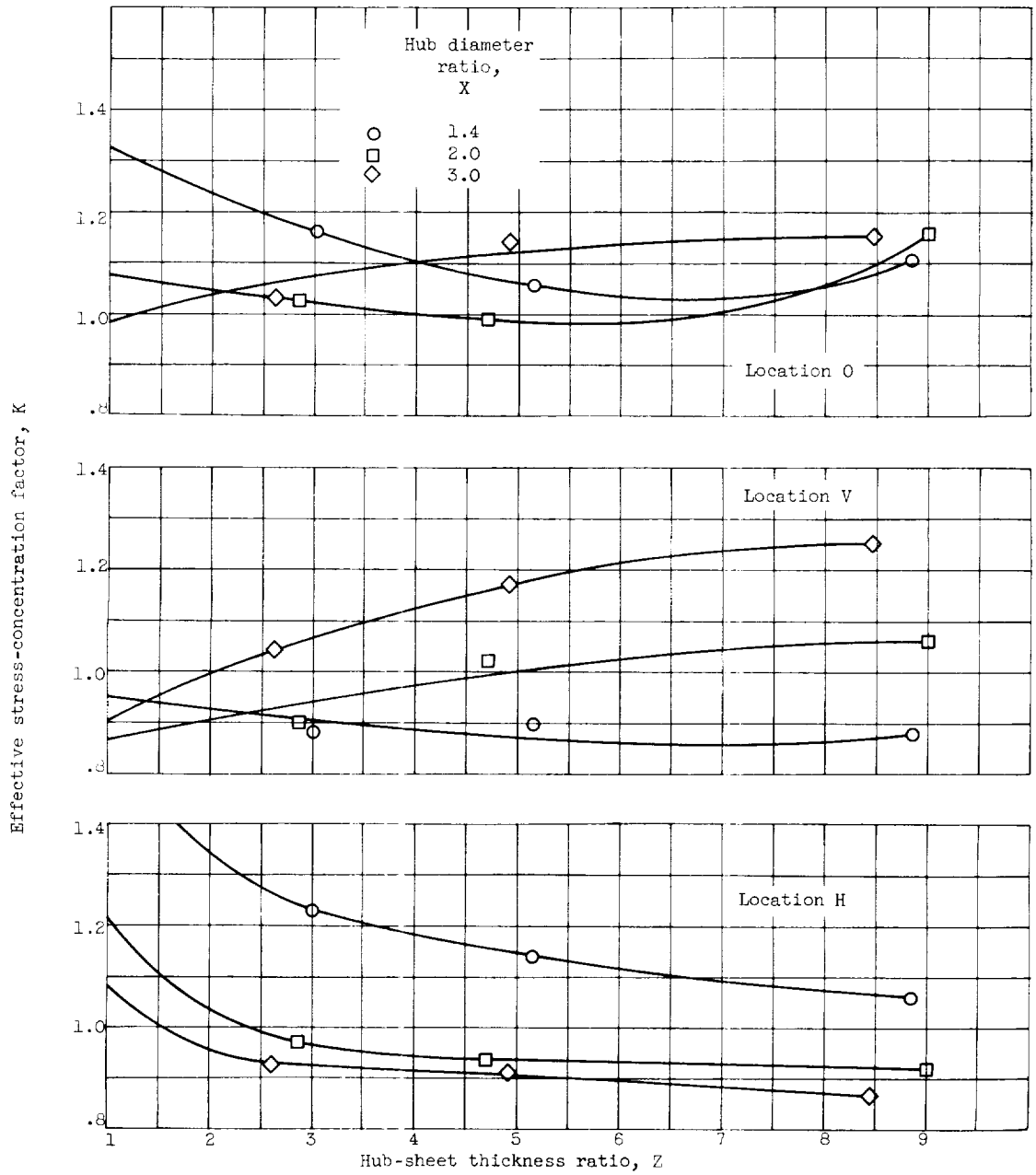

(b) Stress-field ratio, 1.5:1.

Figure 4. - Continued. Effective stress-concentration factors in sheet.

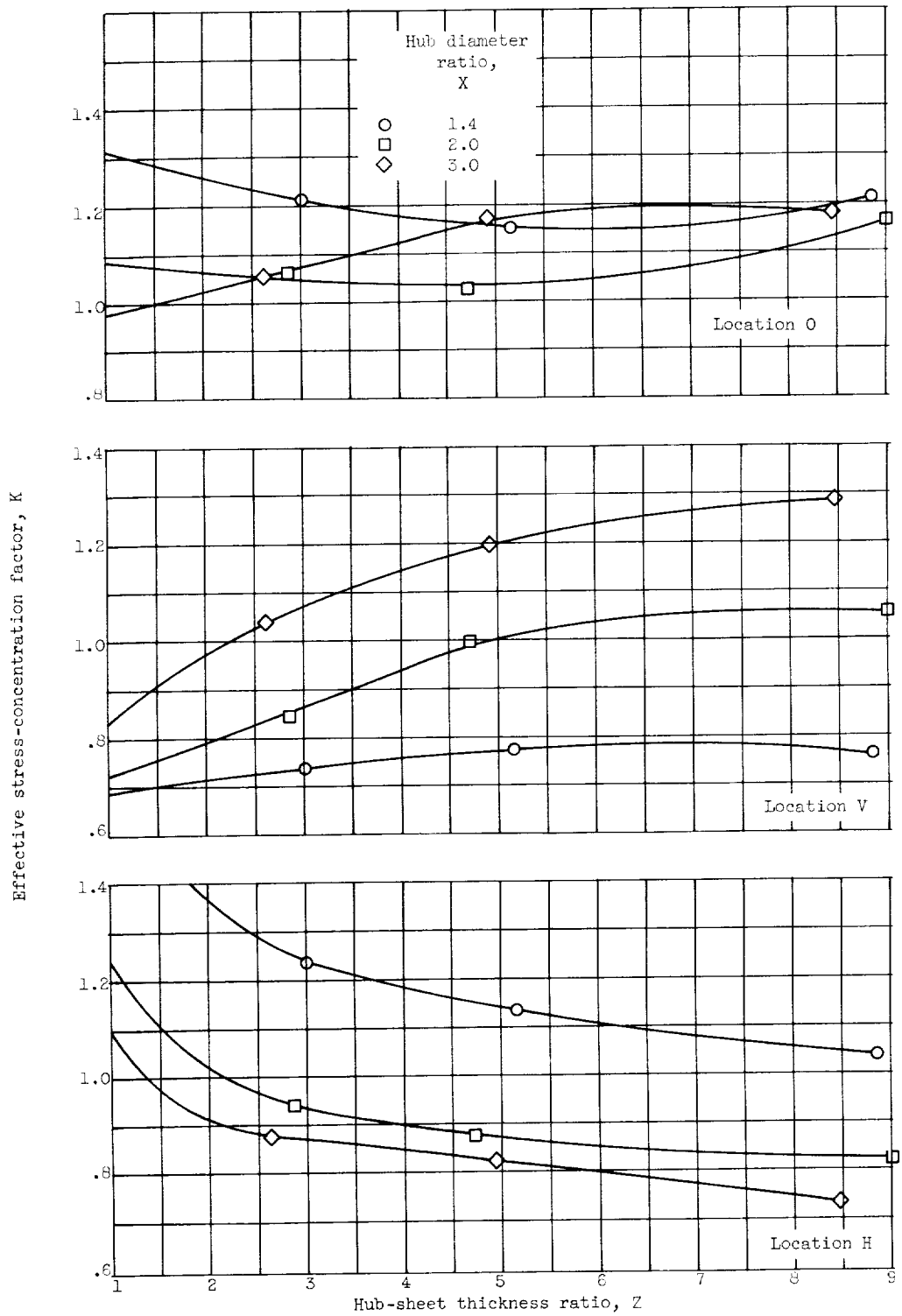

(c) Stress-field ratio, 2:1.

Figure 4. - Continued. Effective stress-concentration factors in sheet.

E-1362

E-1362

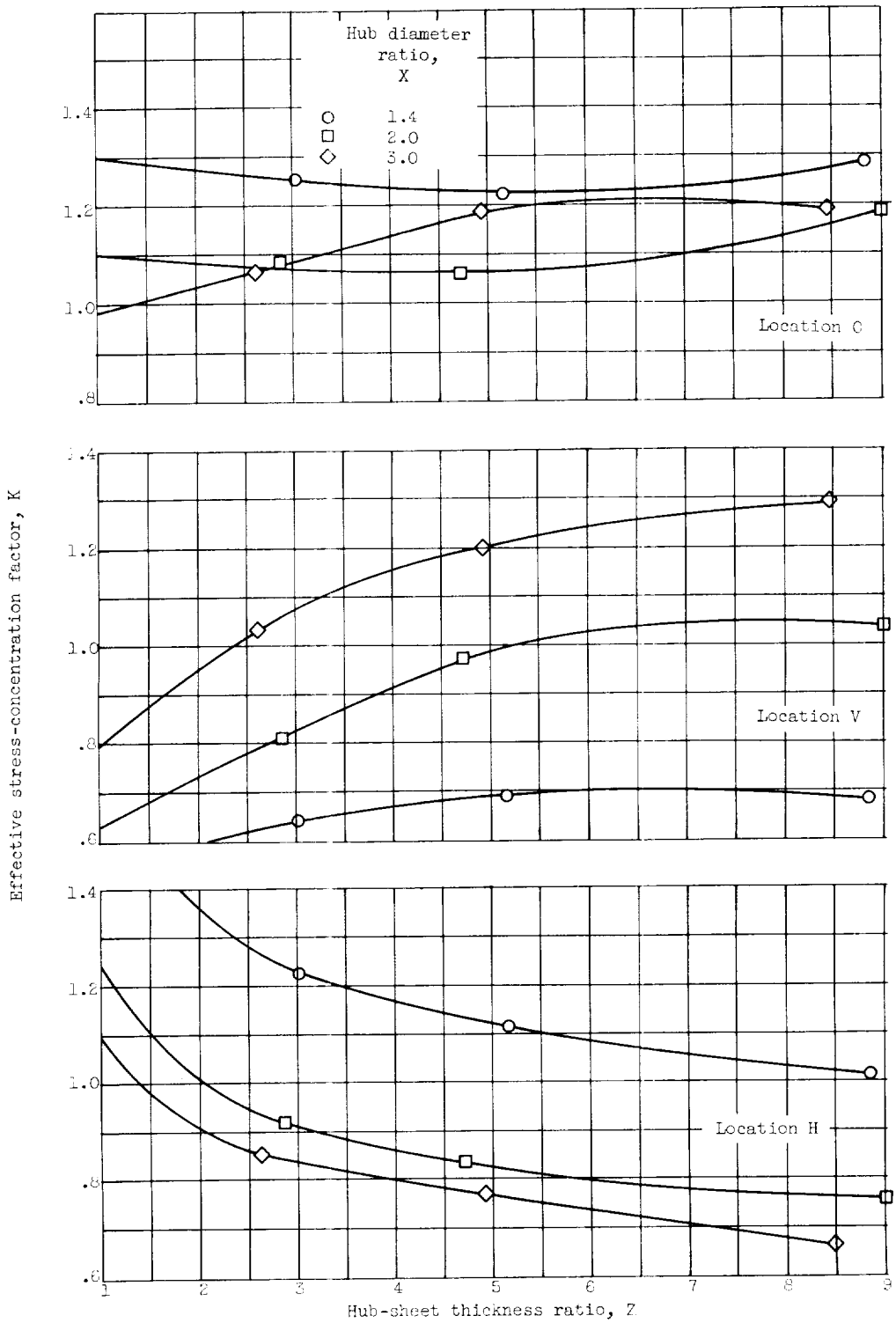

(d) Stress-field ratio, 2.5:1.

Figure 4. - Concluded. Effective stress-concentration factors in sheet.

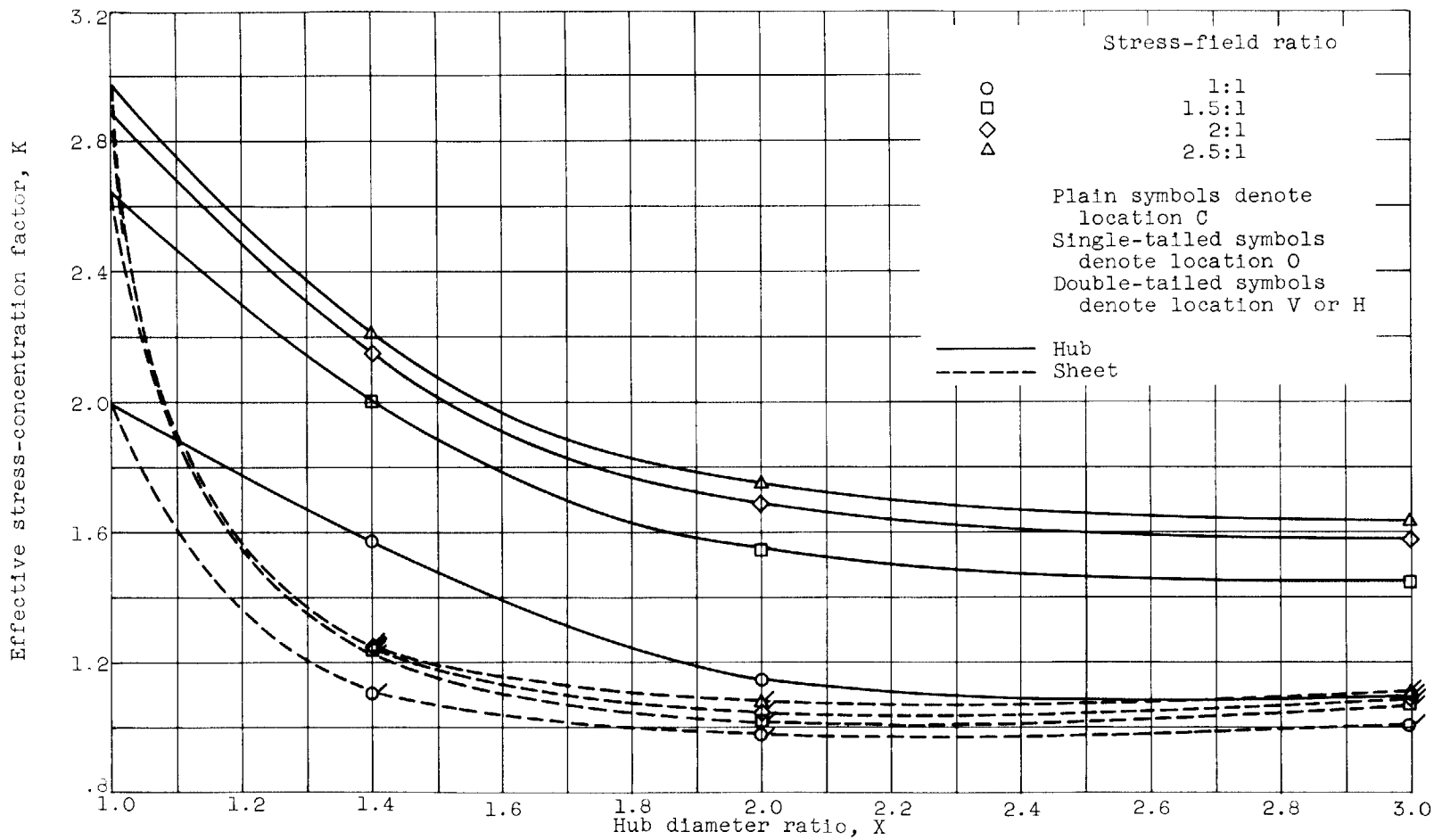

(a) Hub-sheet thickness ratio Z, 3.

Figure 5. - Effect of reinforcement outer diameter on maximum effective stress-concentration factor in sheet and hub.

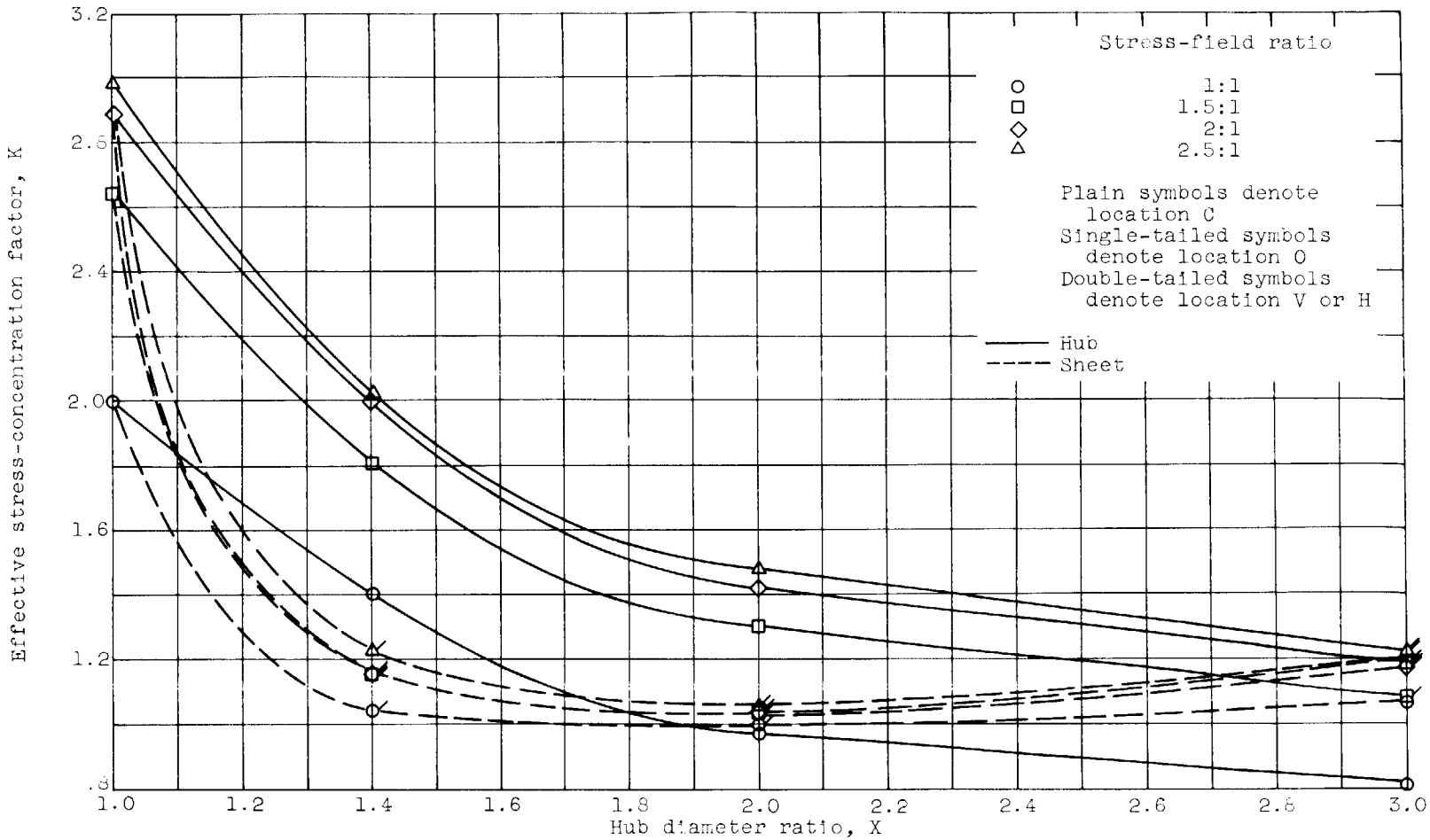

(b) Hub-sheet thickness ratio Z, 5.

Figure 5. - Continued. Effect of reinforcement outer diameter on maximum effective stress-concentration factor in sheet and hub.

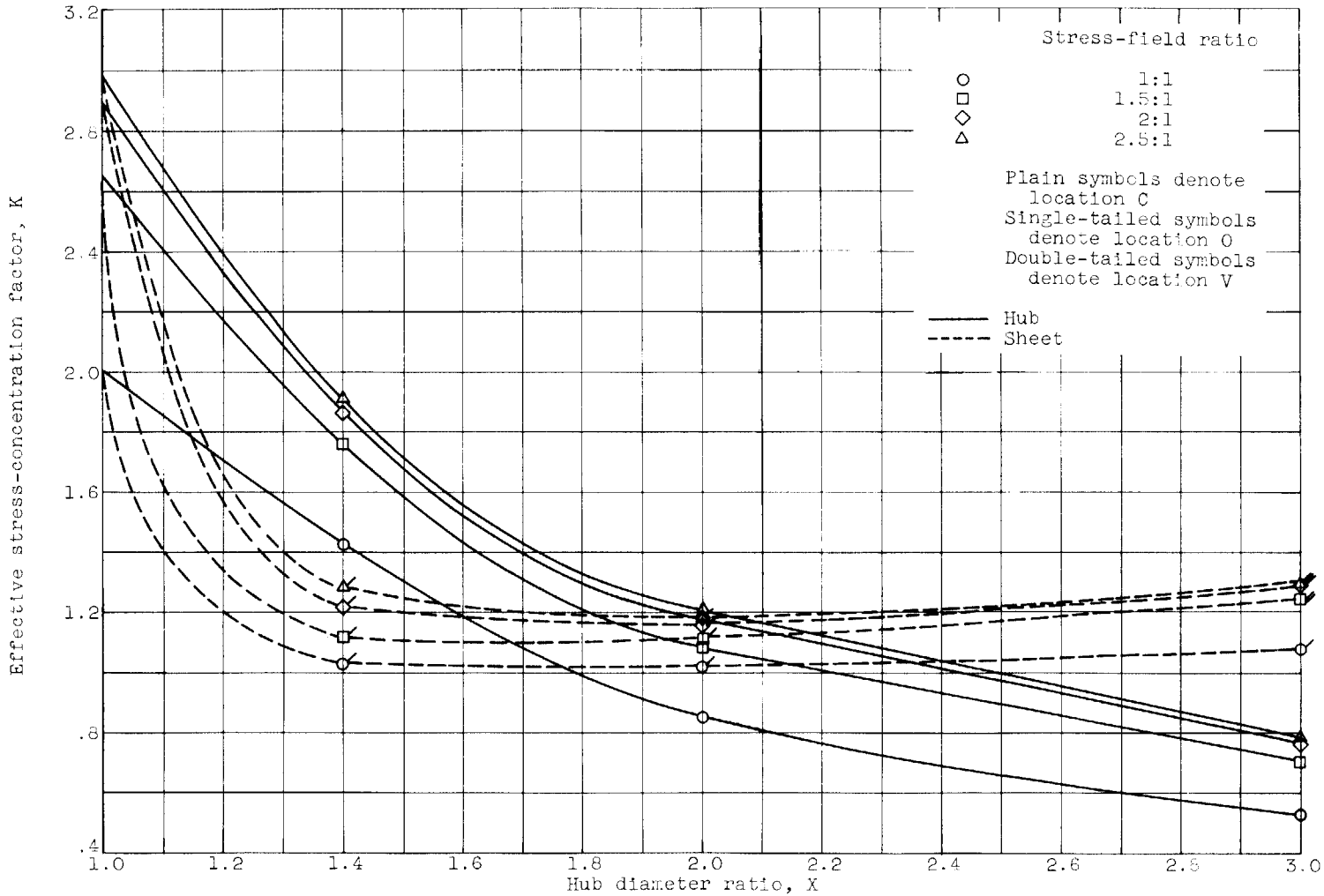

(c) Hub-sheet thickness ratio Z, 9.

Figure 5. - Concluded. Effect of reinforcement outer diameter on maximum effective stress-concentration factor in sheet and hub.

E-1362

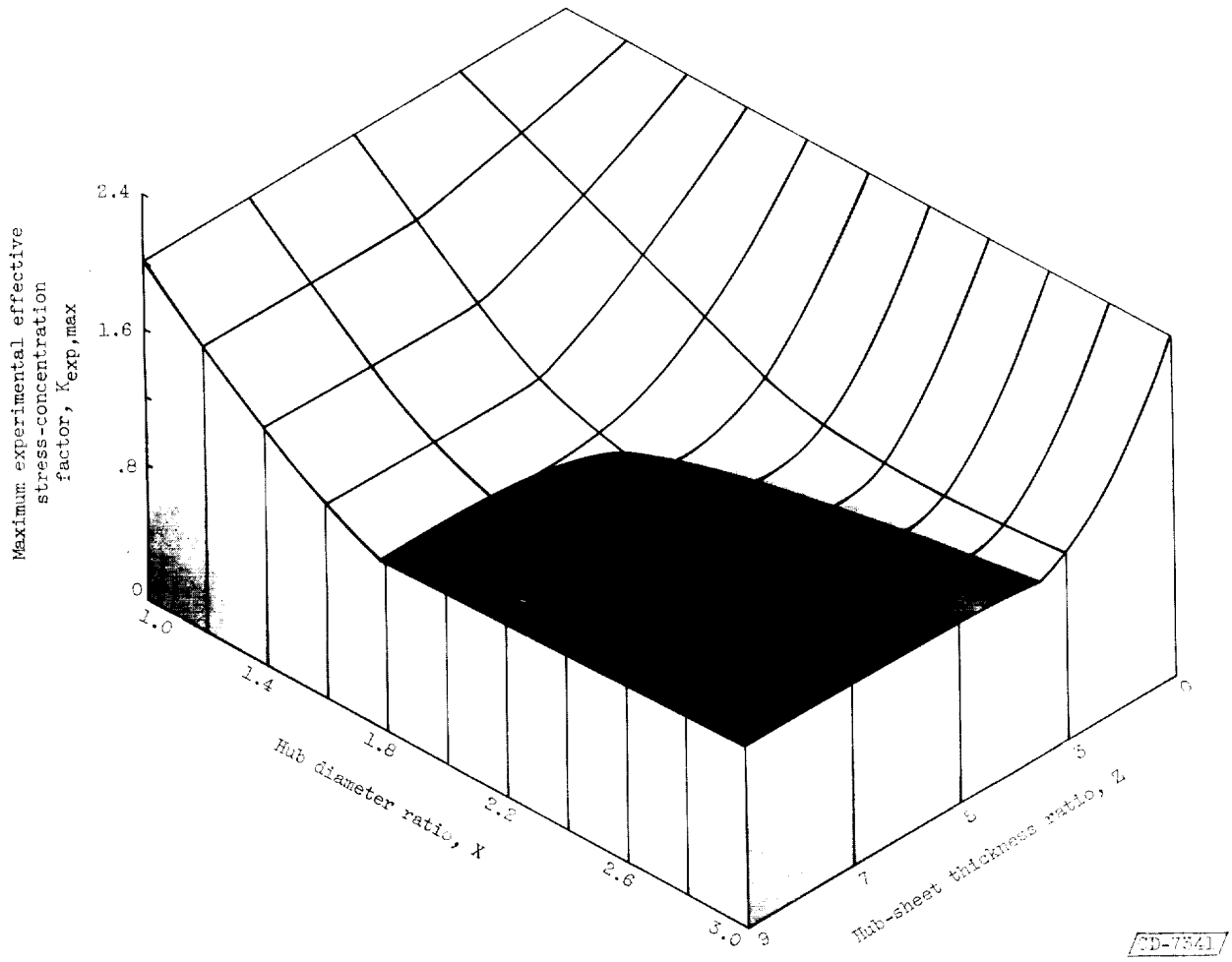

(a) Stress-field ratio, 1:1.

Figure 6. - Maximum experimental effective stress-concentration factor plotted against hub diameter ratio X and hub-sheet thickness ratio Z.

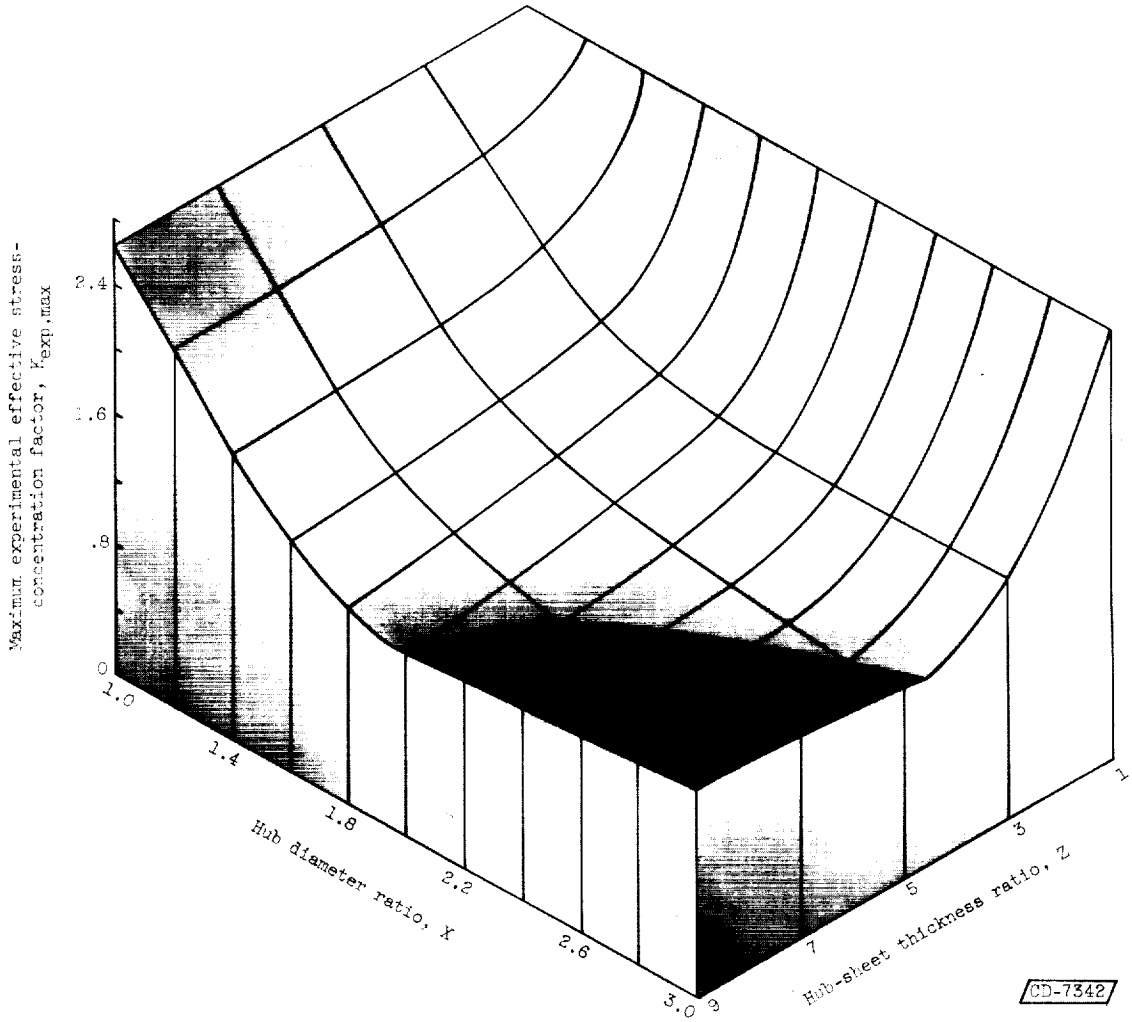

(b) Stress-field ratio, 1.5:1.

Figure 6. - Continued. Maximum experimental effective stress-concentration factor plotted against hub diameter ratio X and hub-sheet thickness ratio Z.

E-1362

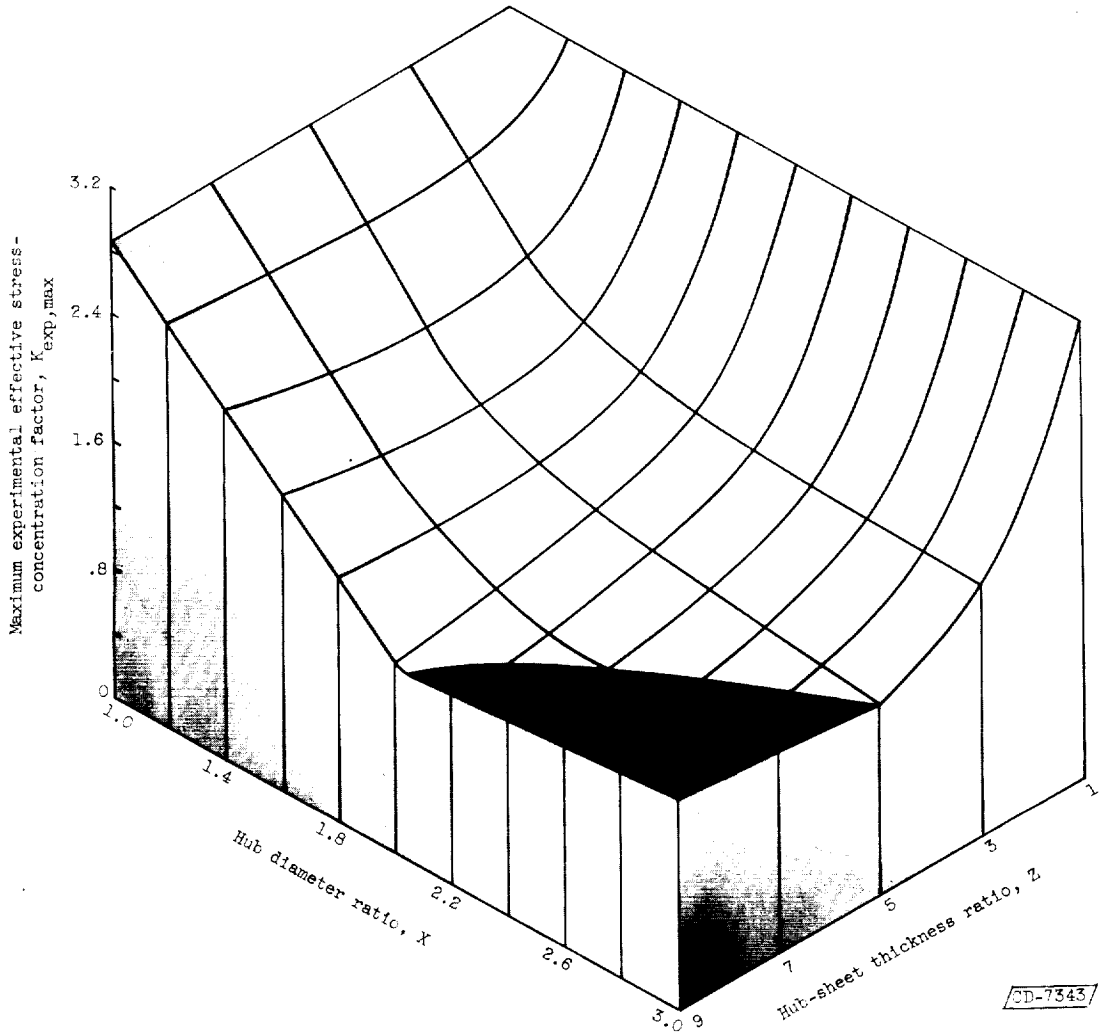

(c) Stress-field ratio, 2:1.

Figure 6. - Continued. Maximum experimental effective stress-concentration factor plotted against hub diameter ratio X and hub-sheet thickness ratio Z.

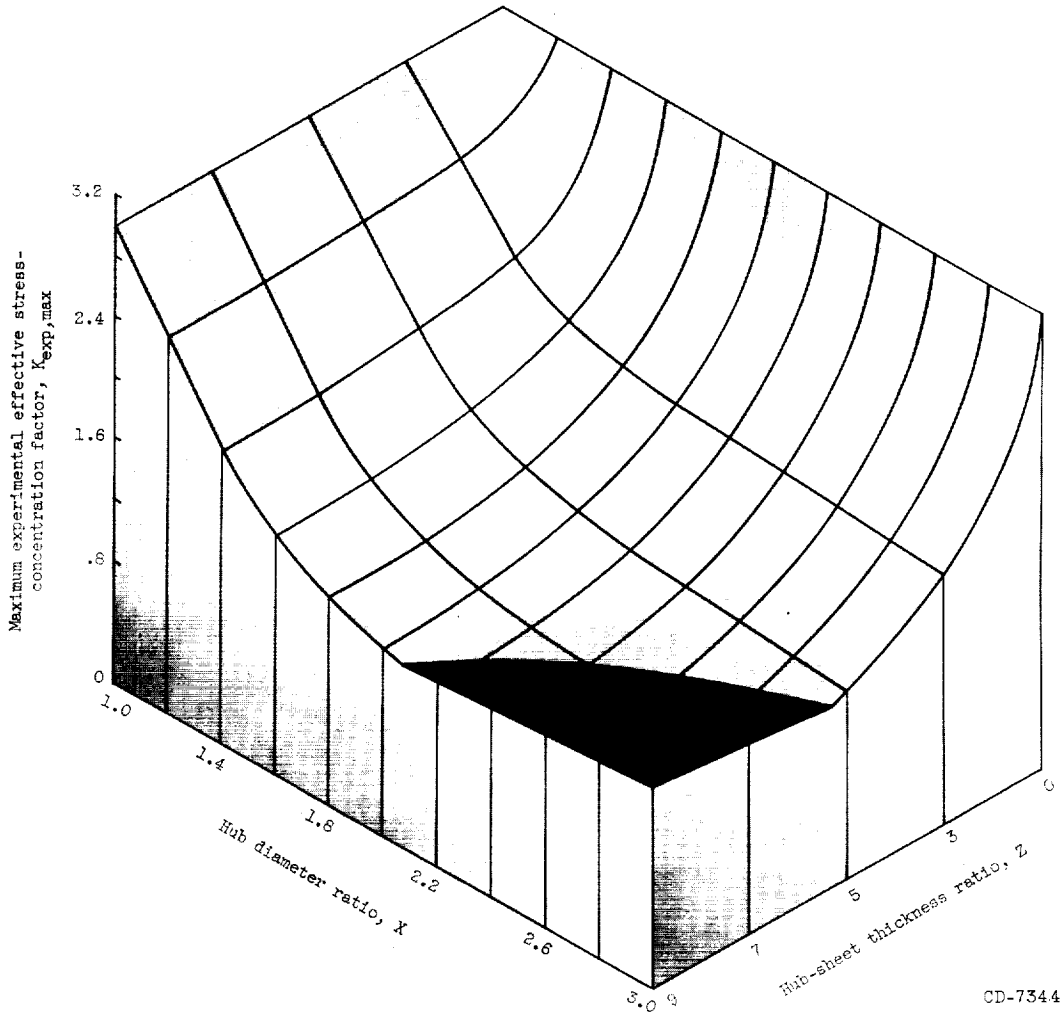

(d) Stress-field ratio, 2.5:1.

Figure 6. - Concluded. Maximum experimental effective stress-concentration factor plotted against hub diameter ratio X and hub-sheet thickness ratio Z.

E-1362

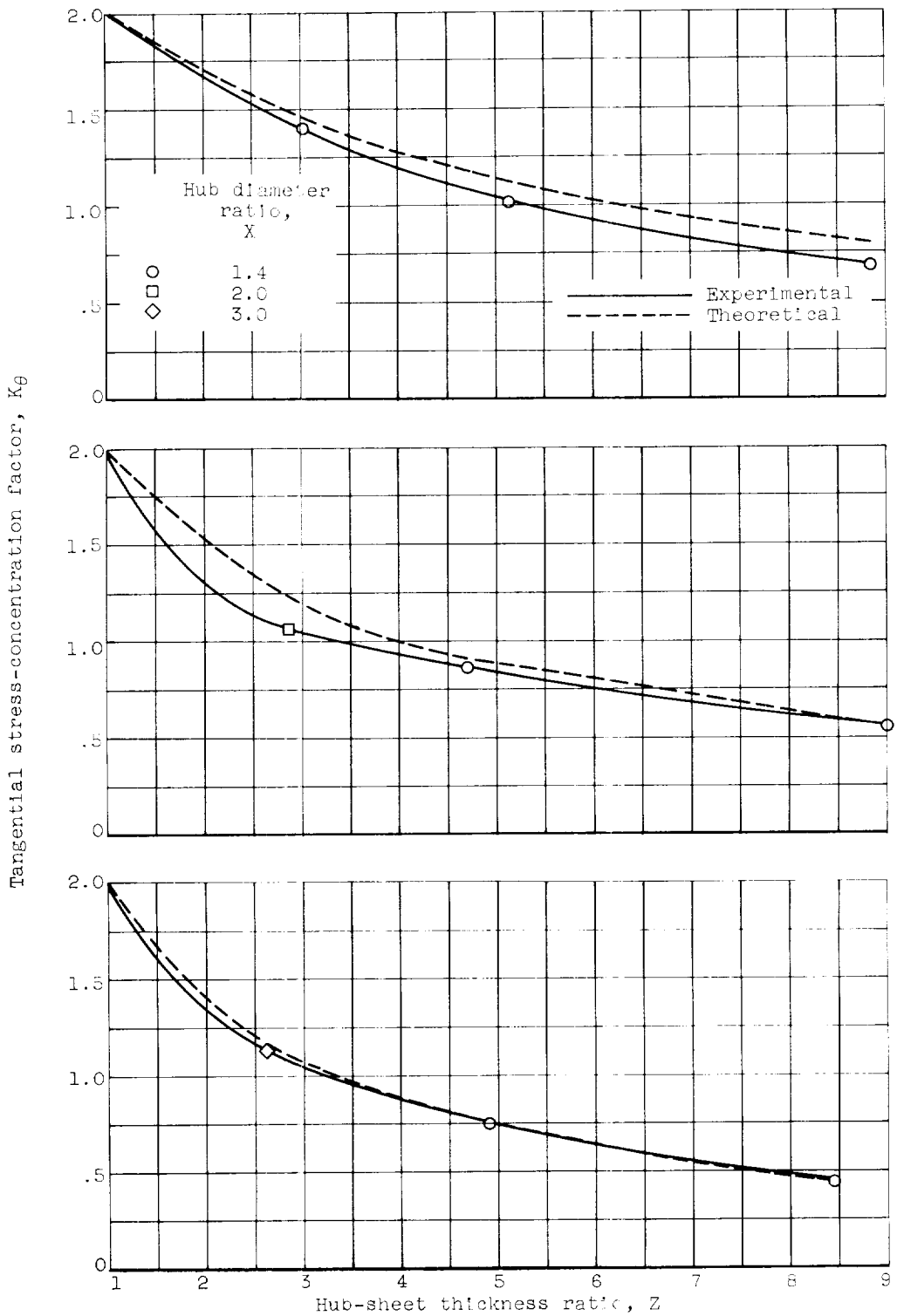

Figure 7. - Comparison of experimental and theoretical tangential stress-concentration factors at location C for 1:1 stress-field ratio.

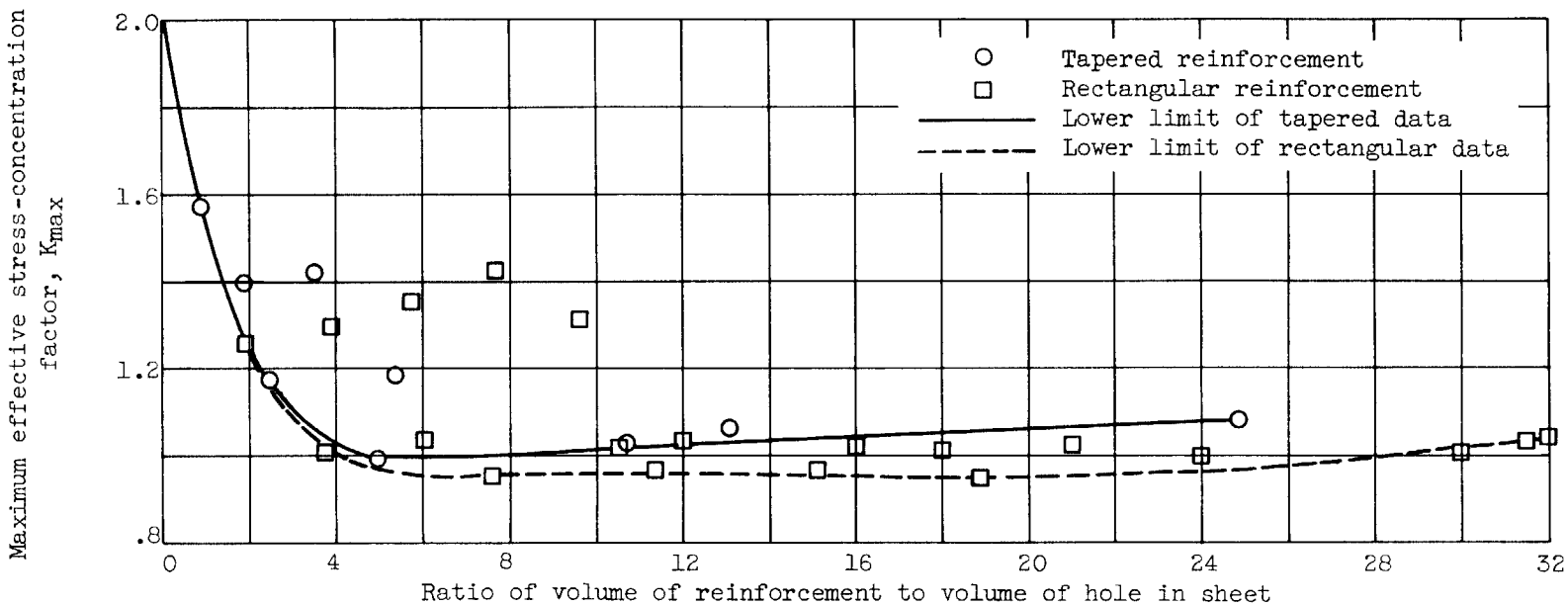

(a) Stress-field ratio, 1:1.

Figure 8. - Comparison of rectangular and tapered reinforcements on volume basis.

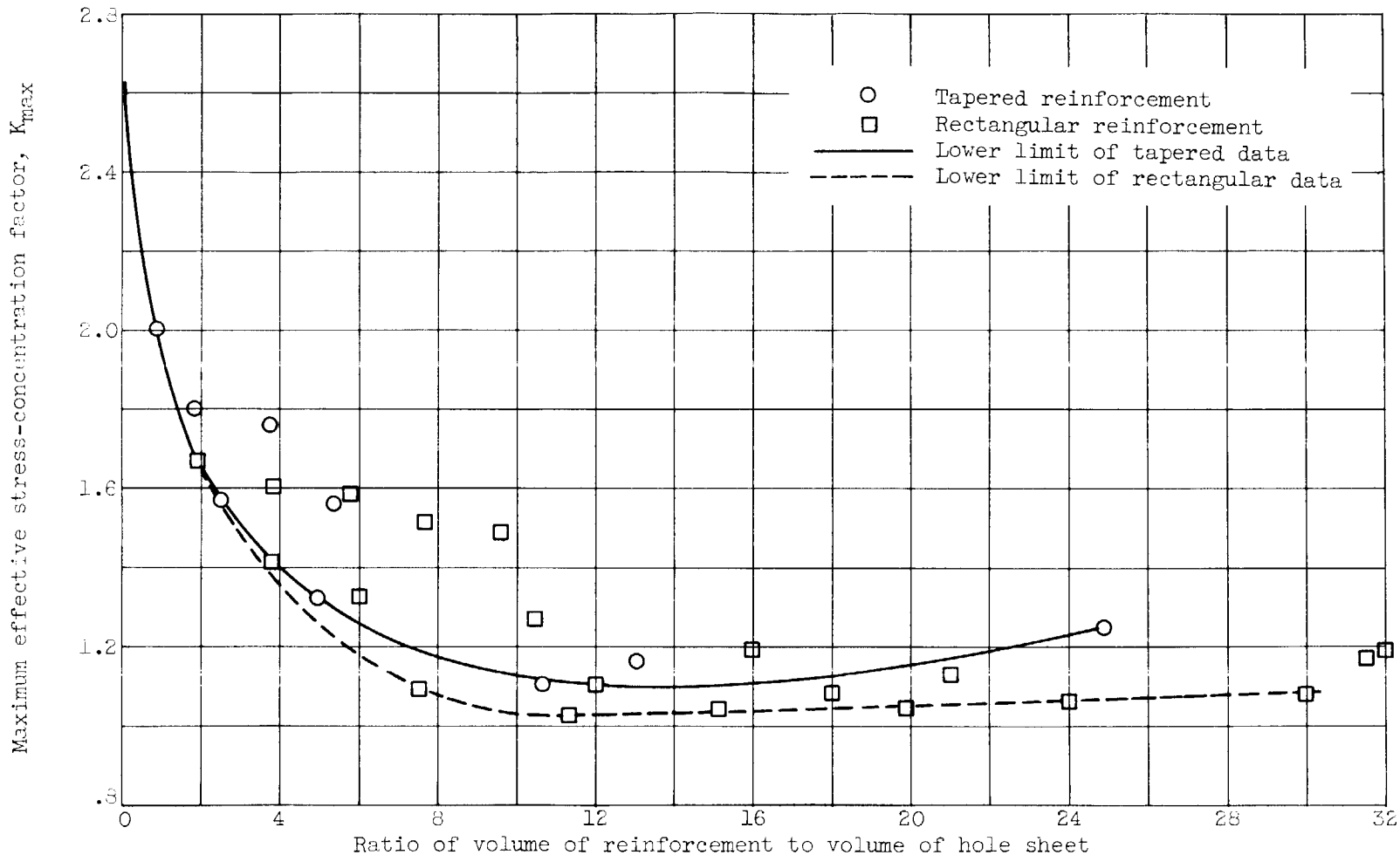

(b) Stress-field ratio, 1.5:1.

Figure 8. - Continued. Comparison of rectangular and tapered reinforcements on volume basis.

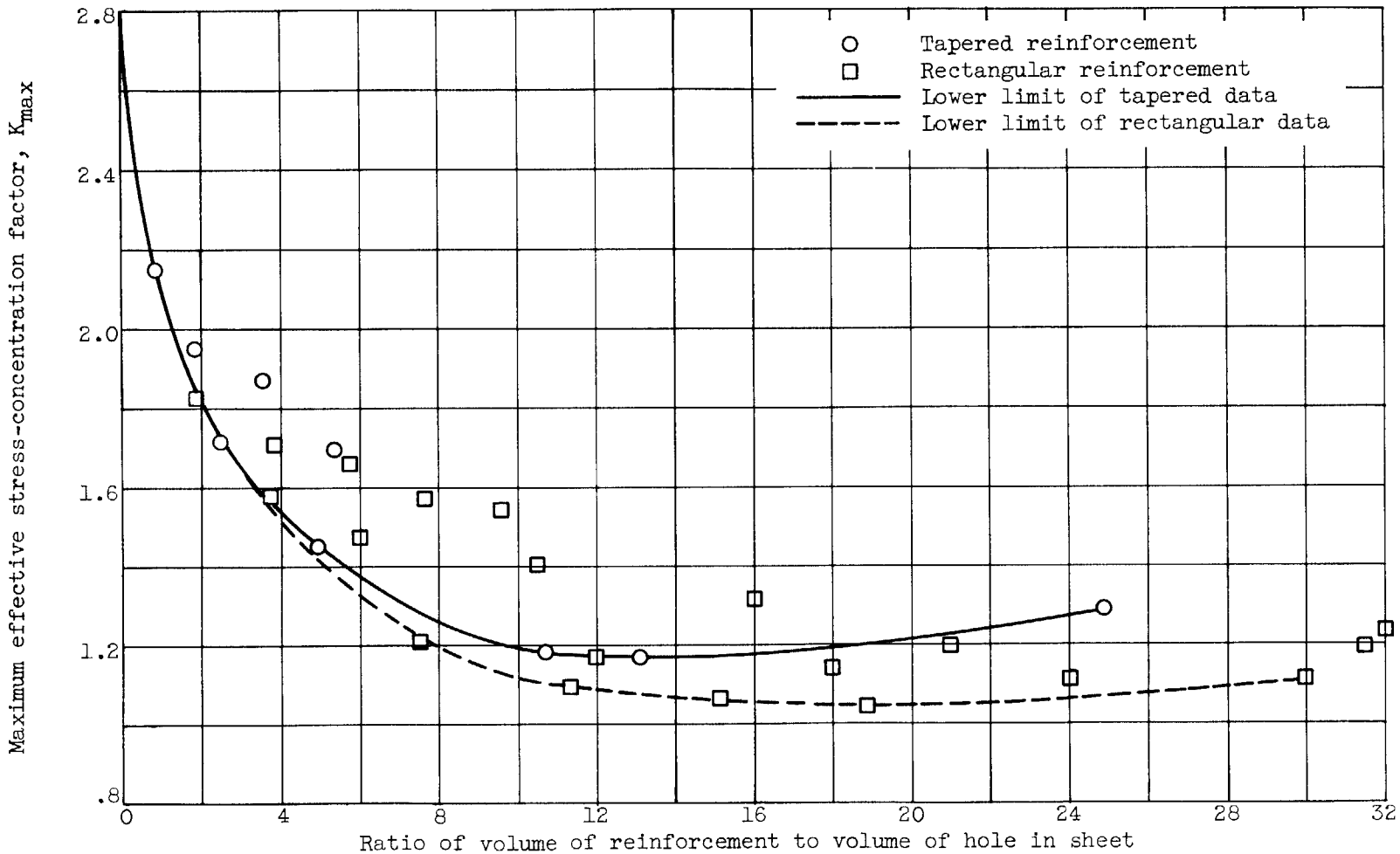

(c) Stress-field ratio, 2:1.

Figure 8. - Continued. Comparison of rectangular and tapered reinforcements on volume basis.

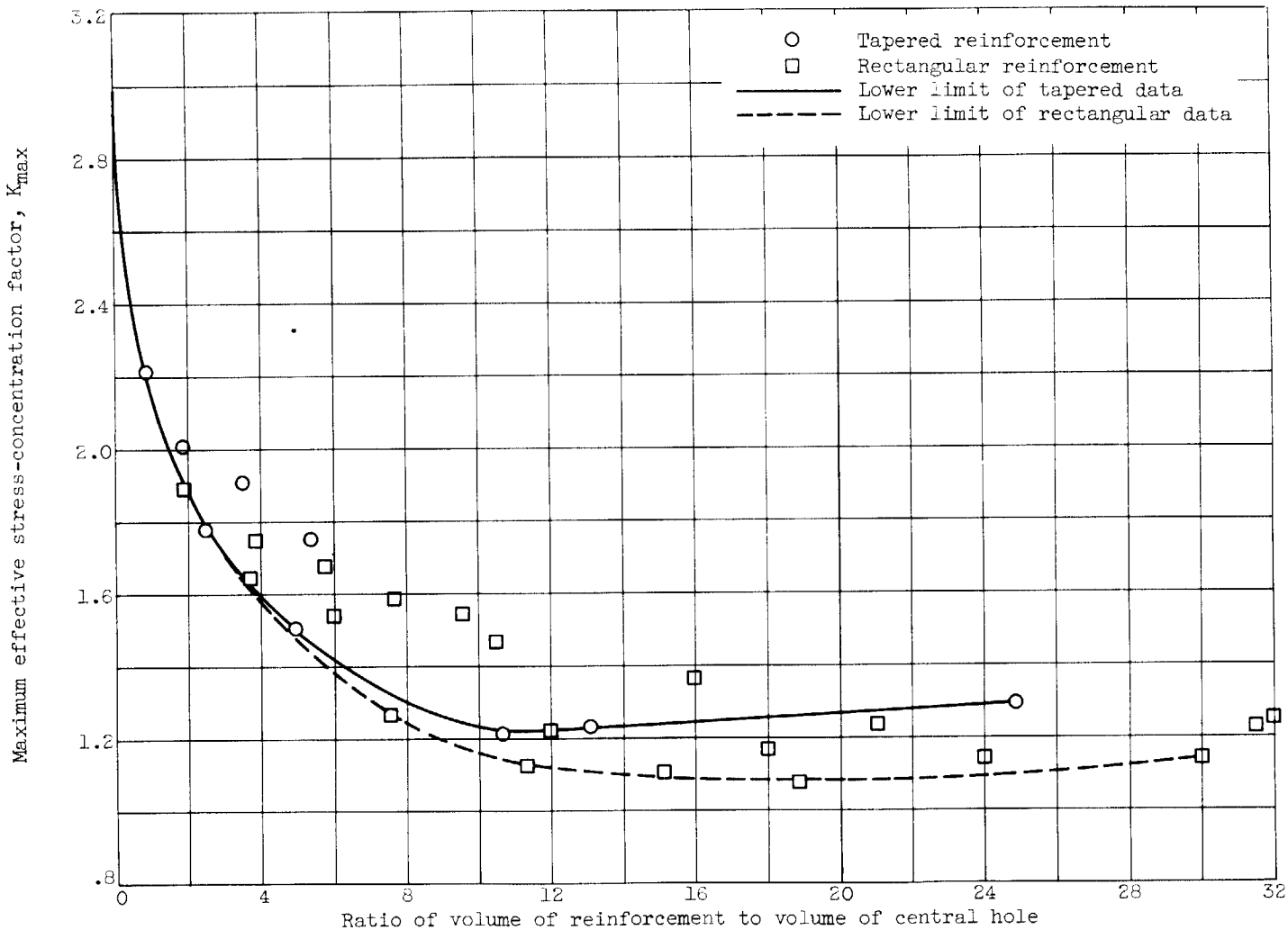

(d) Stress-field ratio, 2.5:1.

Figure 8. - Concluded. Comparison of rectangular and tapered reinforcements on volume basis.

NASA-Langley, 1962 E-1362